# Bending of MgO tubes: Mechanically induced hexagonal phase of magnesium oxide

Andrey N. Enyashin,[1,2] Igor R. Shein,[1,*] and Alexander L. Ivanovskii[1]
[1]*Institute of Solid State Chemistry, Ural Branch of the Russian Academy of Sciences, 620041 Ekaterinburg, Russia*
[2]*Physical Chemistry, Technische Universität Dresden, D-01062 Dresden, Germany*
(Received 27 January 2007; revised manuscript received 26 March 2007; published 29 May 2007)

The present work constitutes a study of the response of magnesium oxide nanotubes on the bend deformation. Our molecular-dynamics simulations show that the structure of the MgO tubes being face centered cubic at ambient conditions is transformed under mechanically induced buckling stress to hexagonal near the tube bend. This transformation occurs through a break of the Mg-O bonds between two adjacent $Mg_2O_2$ tetragons and the formation of $Mg_3O_3$ hexagons. *Ab initio* density-functional band-structure calculations were performed to predict the structural and electronic properties of hexagonal MgO phase and to compare with those for the cubic *B*1 and *B*2 MgO phases.

DOI: 10.1103/PhysRevB.75.193408 PACS number(s): 62.25.+g, 64.60.My

The study of mechanical behavior of nanotubes (NTs) is exceedingly important from the standpoint of possible applications for the engineering of nanotube-based devices such as scanning probes, electronic transistors, etc.[1] A variety of experimental and theoretical methods has been used to investigate the mechanical properties of inorganics, and especially carbon nanotubes (C-NTs), and to understand their mechanical behavior in the elastic regime, see reviews.[2–4]

Recently, some progress has also been attained in the examination of the stress-induced effects outside of the elastic limit.[5–9] Among them, the local structural reconstruction of the tube wall, which is tantamount to a local phase transformation of the nanotubular material, seems to be very interesting. They allow a fabrication of the different mechanically controlled types of heterojunctions containing within tube walls the local inclusions of various nanophases with high engineering potential. For carbon and other graphitelike tubes, such structural transitions may be caused by the formation of topological defects.[2–4] For example, in the C-NTs, such defects are the presence of the pentagons and heptagons in the wall structure of ideal helical nanotubes (the so-called Stone-Wales transformation[10]), which can lead to an essential change of their electronic properties.[11–13]

The discovery of the metal oxide nanotubes has continued a rapid development in the field of nanoscale materials. The numerous important applications of oxides together with the intrinsic multifunctionality specific to the tubular quasi-one-dimensional (1D) structures have attracted a great interest in both scientific and technological areas and have brought an effort to the synthesis and exploration of oxide NTs.[14–17] Meanwhile, the data about the mechanical behavior of metal oxide tubes and the stress effect on the properties of oxide 1D structures are very limited.

Here, we focus on the study of a possibility to achieve the mechanically induced structural transitions in oxide 1D nanostructures and present the results of the computer simulations of magnesium oxide nanotubes. The MgO nanotubes were chosen because plenty of various MgO nanomaterials with great potential applications have been successfully fabricated up to now, such as nanowires, nanotubes, nanoflowers, nanocables, nanocubes, nanopolyhedra, etc.[18–22] The synthesis methods were proposed for the preparation of MgO nanomaterials with different morphologies based on these structures.[22,23] In turn, the crystalline MgO with its superior chemical inertness, mechanical hardness, and small positive electron affinity is a widely used functional material. Note that (i) MgO is crystallized in the simple *cubic B*1 (NaCl-type) structure at ambient conditions and its pressure-induced phase transition to other cubic *B*2 (CsCl type) was predicted (see, for example, Ref. 23, and references therein) and (ii) all known magnesium oxide nanosystems[18–22] also adopt the cubic structure.

In this Brief Report, we show that the structure of the cubic MgO tubes under mechanically induced buckling stress can be transformed to hexagonal within the area of the tube bend. Using *ab initio* density-functional band-structure calculations, we consider the structural and electronic properties of hexagonal MgO phase in comparison with those for the known cubic (*B*1 and *B*2) MgO phases.

Since the synthesized MgO tubes have a fcc structure and exhibit prismatic morphology[18,22] with both interior and exterior polygonal cross sections for a starting model of the MgO tubes, we choose a square-prismatic hollow structure (see Fig. 1) composed from three (001) atomic sheets of crystalline magnesium oxide, as described in Ref. 24. The length of the tube fragment is $L_0=12.6$ nm and the number of atoms is $N=5040$. The initial atomic structure of the MgO NT was optimized by the molecular mechanics method such that the total energy is minimized up to $10^{-4}$ eV and the forces between atoms are close to zero. We found that the optimized tube retains the shape of the starting square-prismatic atomic model, Fig. 1.

The molecular-dynamics (MD) simulations of the response of the tube on the bending deformation were per-

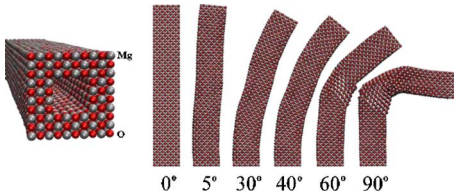


FIG. 1. (Color online) Left: Atomic model of square-prismatic MgO nanotube. Right: The snapshots showing the evolution of the MgO tube under bending ($\theta=0°-90°$) at $T=300$ K.

 

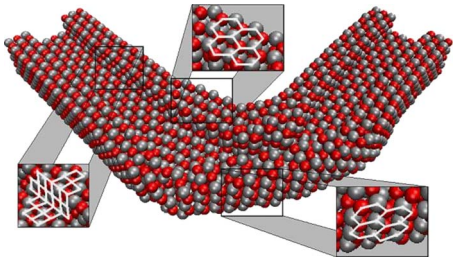

FIG. 2. (Color online) Atomic configurations within the intersected fragment of MgO tube, which illustrate the local structural transition from cubic to noncubic (hexagonal) atomic structure of the tube wall in the bend area.

formed by the following procedure. One end of the tube including 168-atom cell was fixed and the MgO NT was loaded to bend via displacement of other 168-atomic cell at the opposite end of the tube with bending angle $\theta$, which was varied with step, $\Delta\theta=1°$ up to $\theta=90°$. For each displacement, the deformed configuration of the MgO NT was optimized by MD to minimize the potential energy of the system. For the calculations, we employed the same effective pair potential (EPP) method as described previously[24] with the parameters of the pair interaction potentials proposed by Lewis and Catlow.[25] The deformation behavior of the MgO NTs was investigated using MD simulations under conditions of a constant volume and a constant temperature ($T=300$ K, an *NVT* ensemble). All the MD calculations included 5000 iterations and the time step was equal to 2 fs.

The main stages of the MgO NT deformation in the bending process are shown in Fig. 1. One can see the two-step process of the tube deformation. First, for small bending angles $\theta$ from 0° to 35°, the tube undergoes only elastic deformation, where interatomic bonds become compressed or elongated when retaining the cubic wall structure. The most interesting is the next stage for $\theta>40°$, when the limit of elastic behavior of the tube is achieved at a critical stress. Further growth of the deformation leads to a structural mechanism of minimization of the potential energy of the buckling stress that arises through extensive atomic reorganization within the tube walls. As it can be seen in Fig. 1, for deformed tube, this relaxation occurs due to the formation of a local wall site with a *noncubic* structure in the area of the tube bend, and this process is followed by equilibration of the staying tube fragments with a cubic structure.

The detailed analysis shows that this structural transition proceeds due to the break of the common Mg-O bond of two adjacent $Mg_2O_2$ tetragons with their transformation into $Mg_3O_3$ hexagon. These $Mg_3O_3$ hexagons are assembled forming the local segment with a hexagonal BN-like structure. This local atomic rearrangement in the tube walls with the formation of the mechanically induced hexagonal MgO nanophase may be clearly seen in Fig. 2, where an intersected fragment of the MgO tube with an inclusion of the hexagonal-like sites is depicted. Note that the size of the hexagonal-like domain of MgO NT wall grows with increasing deformation load, Fig. 1.

Thus, a type of MgO nanotubes may be produced under mechanically induced bending, which contain an inclusion of the sites with a metastable hexagonal-like wall structure between adjacent cubic fragments. This reveal should be of obvious interest for fabrication of various mechanically controlled types of heterojunctions based on cubic MgO tubes with local inclusions in their walls of noncubic phases.

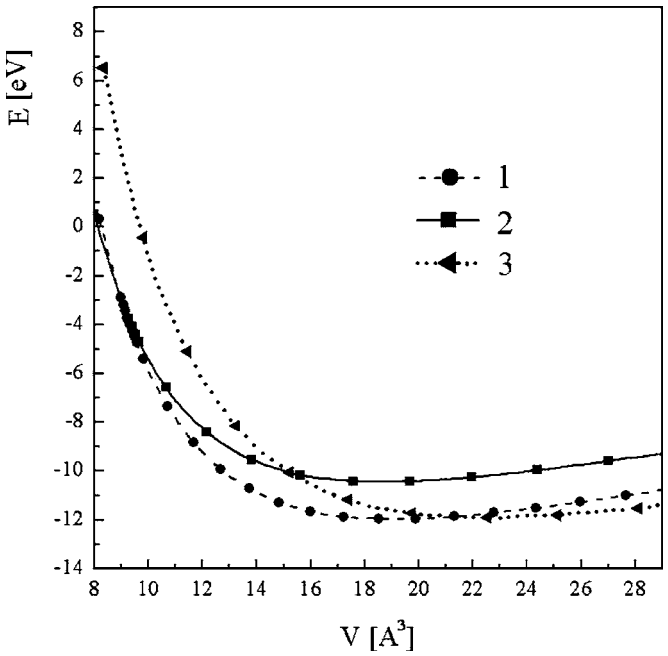


FIG. 3. Total energy *versus* the volume for cubic (1) $B1$, (2) $B2$, and (3) hexagonal-like MgO phases.

To predict the electronic properties of the hexagonal-like MgO phase ($h$-MgO), we performed the band-structure calculations of $h$-MgO and known cubic $B1$ and $B2$ MgO phases. Our calculations based on the density-functional theory (DFT) were performed using the Vienna *ab initio* simulation package VASP (Refs. 26 and 27) in project augmented wave (PAW) formalism.[28,29] Exchange and correlation were described by the Perdew-Zunger functional,[30] adding a nonlocal correction in the form of the generalized gradient approximation (GGA).[31] The calculations for all MgO phases were carried out using a $16\times16\times16$ $k$-point sampling grid and a kinetic-energy cutoff of 500 eV for the expansion of valence orbitals in the plane waves that was shown to be sufficient for the total-energy calculations with a convergence of less than 0.0004 eV/f.u. The core orbitals were considered as frozen within the PAW formalism and the atomic bases for PAW are (Mg) $3s^23p^0$ and (oxygen) $2s^22p^4$. To fit the total energy and to determine the equilibrium lattice constants, we used the Birch-Murnaghan equation of state.[32] Fitting was performed using total energies at 20 different volumes ranging from 0.6 to $1.3V_0$. It should be noted that for the $h$-MgO, independent parameters $a$ and $c$ were fully optimized.

Figure 3 shows the total energy versus the atomic volume for the MgO structures. It is seen that the $B1$ structure is the most stable. The common tangent between the $B1$ and the $B2$ curves determines the transition path between both structures. The calculated transition pressure $B1\rightarrow B2$ $P=443$ GPa is in reasonable agreement with other available

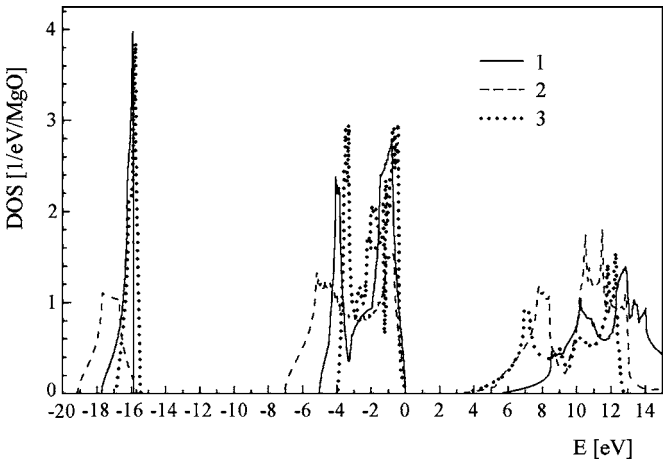


FIG. 4. The electronic density of states for cubic (1) $B1$, (2) $B2$, and (3) hexagonal-like MgO phases.

data,[23] whereas $h$-MgO has a considerably larger volume compared to $B1$ and $B2$ phases, and $B1 \rightarrow h$-MgO transition can be achieved by applying a negative pressure at about −25 GPa. The difference between the minimal energies of the ground states of $B1$ and hexagonal-like phases is at about 0.06 eV per MgO "molecule."

The equilibrium lattice constants are $a=4.2342$ Å ($B1$), $a=5.2954$ Å ($B2$), $a=3.5104$ Å, and $c=4.2219$ Å; $c/a=1.203$ ($h$-MgO). In the $B1$ and $B2$ phases, the Mg and O ions are placed in six- and eightfold positions with equivalent bond lengths $d_{\text{Mg-O}}=2.117$ and 2.293 Å, respectively. For $h$-MgO, the ions adopt an unusual fivefold coordination with $d_{\text{Mg-O}}=2.027$ Å between the nearest-neighbor ions within the hexagonal plane and $d_{\text{Mg-O}}=2.111$ Å between ions in the adjacent layers.

Let us discuss the electronic properties of MgO polymorphs. In Fig. 4, we present the density of states (DOS) for $B1$, $B2$, and $h$-MgO, as obtained by our VASP calculations. Their energy spectra are formed by the low-lying quasicore O $2s$ states separated from the occupied O $2p$ states by a wide gap in agreement with previous data.[33] The bottom of unoccupied conduction band consists mainly of Mg $s,p$ and O $2p$ antibonding states. A very small admixture of magnesium states is found in the valence O $2p$-like band that testifies the ionic bonding between oxygen and magnesium atoms. The changes in the DOSs depending on the structural type and coordination numbers of ions for MgO polymorphs are seen in Fig. 4. According to our calculations, the values of the dielectric gap $E_g$ are 4.52, 2.38, and 3.34 eV for $B1$, $B2$, and $h$-MgO polymorphs, respectively. Despite the well-known[34,35] underestimation of band gap of insulating oxides by the DFT-GGA first-principles band-structure calculations, these results demonstrate the variation $E_g$ in different MgO polymorphs. We found that the dielectric gap of MgO material will decrease at about 1.2 eV at the phase transformation $B1 \rightarrow h$-MgO.

In summary, by means of molecular-dynamics simulations, we showed that the bending of the MgO tubes leads to the formation of unique nanometer-scaled hexagonal MgO phase that is achieved through a break of common Mg-O bond of two adjacent $Mg_2O_2$ tetragons with their transformation into hexagon $Mg_3O_3$. This opens a controlled way to fabricate magnesium oxide nanotubes with modulated wall structures, where the nanometer-scaled noncubic MgO phase tailored under mechanical strain is included in a tube wall.

Using *ab initio* density-functional band-structure calculations, we have predicted the structural and electronic properties of $h$-MgO phase. We showed that the application of negative pressure to the $B1$ phase is a way to stabilize the $h$-MgO phase in a bulk form. Probably, this phase may be prepared under nonequilibrium conditions as thin films were deposited at the surfaces of the corresponding hexagonal-like substrates.

Finally, our estimations of band gaps for $B1$ and $h$-MgO phases concluded that mechanically deformed MgO tubes with a local inclusion of hexagonal-like phase between adjacent cubiclike walls can be assumed as insulator-insulator heterojunction with a decreasing band gap at about 1.2 eV for the bent area. We believe that further study of the structural and electronic properties and conductivity of deformed MgO NTs can be useful for the search of applications of these functional nanomaterials.

Financial support of the Russian Foundation for Scientific Schools Grant No. SS 5138.2006.3 and RFBR (Grants No. 07-03-00026 and 07-03-96061) is gratefully acknowledged. A.N.E. thanks the Foundation of the President of the Russian Federation (Grant No. MK-5126.2006.3).

*Corresponding author. Electronic address: shein@ihim.uran.ru

[1] M. S. Dresselhaus, G. Dresselhaus, and P. C. Eklund, *Science of Fullerenes and Carbon Nanotubes* (Academic, New York, 1996).

[2] D. Qian, G. J. Wagner, W. K. Liu, M.-F. Yu, and R. S. Ruoff, Appl. Mech. Rev. **55**, 495 (2002).

[3] J. Bernholc, D. Brenner, M. B. Nardelli, V. Meunier, and C. Roland, Annu. Rev. Mater. Res. **32**, 347 (2002).

[4] H. Rafii-Tabar, Phys. Rep. **390**, 235 (2004).

[5] T. Belytschko, S. P. Xiao, G. C. Schatz, and R. S. Ruoff, Phys. Rev. B **65**, 235430 (2002).

[6] M. A. L. Marques, H. E. Troiani, M. Miki-Yoshida, M. Jose-Yacaman, and A. Rubio, Nano Lett. **4**, 811 (2004).

[7] S. H. Yeak, T. Y. Ng, and K. M. Liew, Phys. Rev. B **72**, 165401 (2005).

[8] W. Yu, W. X. Xi, and N. Xianggui, Modell. Simul. Mater. Sci. Eng. **12**, 1099 (2004).

[9] K. M. Liew, C. H. Wong, and M. J. Tan, J. Appl. Phys. **99**, 114312 (2006).

[10] G. G. Samsonidze, G. G. Samsonidze, and B. I. Yakobson, Comput. Mater. Sci. **23**, 62 (2002).

[11] J. Cao, Q. Wang, and H. Dai, Phys. Rev. Lett. **90**, 157601 (2003).

[12] Y. Guo and W. Guo, J. Phys. D **36**, 805 (2003).
[13] B. Shan, G. W. Lakatos, S. Peng, and K. Cho, Appl. Phys. Lett. **87**, 173109 (2005).
[14] G. R. Patzke, F. Krumeich, and R. Nesper, Angew. Chem., Int. Ed. **41**, 2446 (2002).
[15] C. N. R. Rao, A. Govindaraj, G. Gundiah, and S. R. C. Vivekchand, Chem. Eng. Sci. **59**, 4665 (2004).
[16] M. Law, J. Goldberger, and P. Yang, Annu. Rev. Mater. Res. **34**, 83 (2004).
[17] S. G. Zakharova, V. L. Volkov, V. V. Ivanovskaya, and A. L. Ivanovskii, Usp. Khim. **74**, 651 (2005).
[18] Y. B. Li, Y. Bando, D. Golberg, and Z. W. Liu, Appl. Phys. Lett. **83**, 999 (2003).
[19] C. Tang, Y. Bando, and T. Sato, J. Phys. Chem. B **106**, 7449 (2002).
[20] X.-S. Fang, C.-H. Ye, T. Xie, Z.-Y. Wang, J.-W. Zhao, and L.-D. Zhang, Appl. Phys. Lett. **88**, 013101 (2006).
[21] Q. Yang, J. Sha, L. Wang, J. Wang, and D. Yang, Mater. Sci. Eng., C **26**, 1097 (2006).
[22] Y. Hao, G. Meng, Y. Zhou, M. Kong, Q. Wei, M. Ye, and L. Zhang, Nanotechnology **17**, 5006 (2006).
[23] S.-N. Luo, D. C. Swift, R. N. Mulford, N. D. Drummond, and G. J. Ackland, J. Phys.: Condens. Matter **16**, 5435 (2004).
[24] A. N. Enyashin, G. Seifert, and A. L. Ivanovskii, Phys. Solid State **48**, 801 (2006).
[25] G. V. Lewis and C. R. A. Catlow, J. Phys. C **18**, 1149 (1985).
[26] G. Kresse and J. Hafner, Phys. Rev. B **47**, 558 (1993).
[27] G. Kresse and J. Furthmuller, Phys. Rev. B **54**, 11169 (1996).
[28] D. Vanderbilt, Phys. Rev. B **41**, 7892 (1990).
[29] G. Kresse and J. Hafner, J. Phys.: Condens. Matter **6**, 8245 (1996).
[30] J. P. Perdew and A. Zunger, Phys. Rev. B **23**, 5048 (1981).
[31] J. P. Perdew and Y. Wang, Phys. Rev. B **45**, 13244 (1992).
[32] L.-P. Poirier, *Introduction to the Physics of the Earth's Interior* (Cambridge University Press, Cambridge, 1991).
[33] A. Yamasaki and T. Fujiwara, Phys. Rev. B **66**, 245108 (2002), and references therein.
[34] L. J. Sham and M. Schluter, Phys. Rev. Lett. **51**, 1888 (1983).
[35] J. Robertson, K. Xiong, and S. J. Clark, Thin Solid Films **496**, 1 (2006).